Supplementary Material:
Optimal Counterfactual Explanations in Tree Ensembles

Axel Parmentier [1] **Thibaut Vidal** [2 3]

1. Proofs

Proof of Theorem 1.
Let $\boldsymbol{\lambda}, \boldsymbol{y}$ be a solution of Equations (8–12). We will prove by induction on the depth d that every node v of depth d in every tree $t \in \mathcal{T}$ is such that the variables y_{vt} belong to $\{0, 1\}$ and that there is a unique node v in t at depth d such that $y_v = 1$. Equation (8) gives the result for $d = 1$. Now, suppose that the result is true up to depth d and let v be a node of depth $d + 1$ in some tree t of the forest. Let u be the parent of v. By induction hypothesis, y_u belongs to $\{0, 1\}$. If $y_u = 0$, then Equation (9) implies that $y_v = 0$. If $y_u = 1$, then $y_v = 1$ if $\lambda_{td} = 1$ (resp. 0) and v is the left (resp. right) child of u, and 0 otherwise. In all cases, we have $y_v \in \{0, 1\}$. Therefore, there is a unique node v in t of depth d such that $y_v = 1$. This concludes the induction step and proves the theorem.

Proof of Theorem 2.

(i) Let $\boldsymbol{\lambda}, \boldsymbol{y}, \boldsymbol{x}, \boldsymbol{\mu}$ be a feasible solution.
We will first prove that the numeric features of this solution are consistent with all splits.
Theorem 1 ensures that $\boldsymbol{y}$ is integral and that in each tree t there is a unique leaf l such that $y_l = 1$. Let P be the path from the root of t to l. A backward induction along P using Equation (9) shows that $y_v = 1$ for every vertex v in P and also implies that $y_v = 0$ for all nodes that are not in P.
Let v be a non-leaf node along P. Let i be the feature of v and j be its split level (i.e., such that $v \in \mathcal{V}^I_{tij}$). If P goes to the left child of v, then Equation (16) ensures that $\mu_i^j = 0$ and Equation (15) ensures that $\mu_i^k = 0$ for any $k > j$. Equation (20) then ensures that $x_i \leq x_i^j$. Otherwise, if P goes to the right child of v, then Equations (17) and (15) ensure that $\mu_i^k = 1$ for any $k < j$. Equation (18) ensures that $\mu_i^j > 0$, and Equation (20) then gives $x_i > x_i^j$. Therefore, by disjunction of cases, x_i is consistent with the split at node v.
If i is a binary feature, then Equations (21–23) immediately ensure that $x_i = 0$ if P goes to the left and $x_i = 1$ otherwise, which gives the consistency. The same reasoning on the $\boldsymbol{\nu}$ gives the consistency for the categorical features.

(ii) This result immediately follows from the fact that the number of variables and constraints is in $\mathcal{O}(N_v)$ and that the only constraints with more than two non-zero coefficients are constraints (10), (13), (20), and (27) with $\mathcal{O}(N_v)$ non-zero terms overall in each case.

(iii) We will use Cui et al. (2015) notations when referring to the OAE formulation. The proof reconstructs a solution of the linear relaxation of OAE from the optimal solution of the linear relaxation of OCEAN. We prove this result when all the features are numeric. The other cases are simpler and derive from a similar proof scheme.

Let $\boldsymbol{\lambda}, \boldsymbol{y}, \boldsymbol{x}, \boldsymbol{\mu}$ be an optimal solution of the linear relaxation of our formulation. We reconstruct a solution of the linear relaxation of OAE as follows. First, remark that OAE's variables $\boldsymbol{\phi}$ and OCEAN's variables $\boldsymbol{y}$ corresponding to tree leaves represent the same quantities. Therefore, given a tree t and a leaf k of t, define

$$\phi_{tk} = y_{tk}$$

[1]CERMICS, École des Ponts Paristech; [2]CIRRELT & SCALE-AI Chair in Data-Driven Supply Chains, Department of Mathematics and Industrial Engineering, Polytechnique Montreal, Canada; [3]Department of Computer Science, Pontifical Catholic University of Rio de Janeiro (PUC-Rio), Brazil. Correspondence to: Thibaut Vidal <thibaut.vidal@cirrelt.ca>.

Supplementary material of the paper "Born-Again Tree Ensembles. *Proceedings of the 37^{th} International Conference on Machine Learning*, Online, PMLR 119, 2020". Copyright 2020 by the author(s).

where the ϕ refer to the variables in OAE. The flow constraints (8)-(9) of OCEAN then immediately imply

$$\sum_{k=1}^{m_t} \phi_{tk} = 1.$$

Let i be a numerical feature and let $\hat{j}_i$ be the index associated with the original value $\hat{x}_i$ in OCEAN (see Section 3.3). OAE has the same splits as OCEAN except for the split level $\hat{j}_i$ corresponding to the original value of $\hat{x}_i$. With this, OCEAN defines variables $\{\mu_i^0, \dots, \mu_i^{k_i}\}$ and OAE defines variables $\{v_{i1}, \dots, v_{in_i}\}$ with $n_i = k_i$.

Now, let us set the following values:

$$v_{ij} = \tilde{\mu}_i^{j-1} - \tilde{\mu}_i^j \quad \text{where} \quad \tilde{\mu}_i^j = \begin{cases} \mu_i^j & \text{if } \mu_i^j > \epsilon \\ 0 & \text{otherwise.} \end{cases} \tag{vars}$$

Summing the values of v_{ij} as defined in Equation (vars), we obtain $\sum_j v_{ij} = \mu_i^0 - \tilde{\mu}_i^{k_i}$. Moreover, observe that μ_i^0 does not intervene in constraints (16) of OCEAN, and $\mu_i^{k_i}$ does not intervene in constraints (17). The convexity of the cost and the optimality of the solution of OCEAN considered then imply that $\mu_i^0 = 1$ and $\mu_i^{k_i} \leq \epsilon$ in an optimal solution of the linear relaxation, and therefore $\tilde{\mu}_i^{k_i} = 0$, in such a way that:

$$\sum_{j=1}^{n_i} v_{ij} = 1.$$

Let us now prove that:

$$\phi_{tk} \leq \sum_{v \in S_{kp}} v, \forall t, \forall k, \forall p \in \pi_{tk}, \tag{dis}$$

which implies (by aggregation) the following constraints of OAE:

$$\phi_{tk} \leq \frac{1}{|\pi_{tk}|} \sum_{p \in \pi_{tk}} \sum_{v \in S_{kp}} v, \forall t, \forall k. \tag{agg}$$

For this, consider a tree t, a leaf k, and a node p on the path to leaf k. Let j_p be the index of the split corresponding to p. Suppose that the path goes to the left at p. Constraint (9) of OCEAN implies that $\phi_{tk} = y_{tk} \leq y_{tl(p)}$. Hence,

$$\sum_{v \in S_{kp}} v = \mu_i^0 - \mu_i^{j_p - 1} = 1 - \mu_i^{j_p - 1},$$

and since $y_{tl(p)} \leq 1 - \mu_i^{j_p - 1}$ by constraint (15) and (16) of OCEAN, we obtain (dis). Suppose now that the path goes to the right at p. Constraint (9) of OCEAN implies that $\phi_{tk} = y_{tk} \leq y_{tr(p)}$. Hence,

$$\sum_{v \in S_{kp}} v = \mu_i^{j_p - 1} - \mu_i^{n_i} = \mu_i^{j_p - 1},$$

and since $y_{tr(p)} \leq \mu_i^{j_p - 1}$ by constraint (17) of OCEAN, we obtain (dis).

Moreover, the majority vote constraints (13) and (14) of OCEAN ensure that the majority vote constraint of OAE is satisfied, and thus the solution built is a feasible solution of OAE.

We finally evaluate the cost of this solution. We place ourselves in the general context of a piecewise linear convex loss function, as in Cui et al. (2015). Define $\ell_i^j = \ell(\hat{x}_i, x_i^j)$, the value of the loss for feature i if the counterfactual value for feature i is x_i^j, where x_i^j is the coordinate of split j for feature i in OCEAN and $1 \leq j \leq n_i$. Defining $x_i^0 = 0$ and $x_i^{n_i+1} = 1$, the objective of OCEAN is:

$$\ell_i^0 + \sum_{j=0}^{n_i} (\ell_i^{j+1} - \ell_i^j) \mu_i^j.$$

Reindexing the sum and using the fact that $\tilde{\mu}_i^0 = 1$ and $\tilde{\mu}_i^{n_i} = 0$, we can rewrite this objective with an error non-greater than the numerical precision ϵ as:

$$\sum_{j=1}^{n_i} \ell_i^j (\tilde{\mu}_i^{j-1} - \tilde{\mu}_i^j).$$

Let b_i^j be the coordinate of the splits for OAE. Finally, let $\hat{j}_i$ be the index of the split of OCEAN corresponding to $\hat{x}_i$. We have $b_i^j = x_i^j$ for $j < \hat{j}_i$, and $b_i^j = x_i^{j+1}$ for $j \geq \hat{j}_i$. Consider now the costs $C_{ij}(\boldsymbol{x}^c)$ in the objective of OAE, which correspond to $\ell(\hat{x}_i, \tilde{x}_i^j)$ where $\tilde{x}_i^j$ is the nearest point of $\hat{x}_i$ in the cell j of OAE. By convexity of the loss, $\tilde{x}_i^j$ is the right extremity of the cell if $j < \hat{j}_i$, the left extremity if $j > \hat{j}_i$ and $\hat{x}_i$ if $j = \hat{j}_i$. Given the index shift between x_i^j and b_i^j in $\hat{x}_i$, we get $C_{ij}(\boldsymbol{x}^c) = \ell(\hat{x}_i, x_i^j) = \ell_i^j$. The value of the objective of OAE for the solution reconstructed is therefore

$$\sum_{j=1}^{n_i} v_{ij} C_{ij} = \sum_{j=1}^{n_i} v_{ij} \ell_i^j = \sum_{j=1}^{n_i} \ell_i^j (\tilde{\mu}_i^{j-1} - \tilde{\mu}_i^j),$$

which is the value of the optimal solution of OCEAN.

In summary, we have built a feasible solution of the linear relaxation OAE whose objective is equal to the value of the linear relaxation of OCEAN. This concludes the proof.

Implied integrality of the x variables for binary features and $\boldsymbol{\nu}$ variables for categorical features. Consider an optimal solution of the continuous relaxation of variables $\boldsymbol{x}$ for binary features and $\boldsymbol{\nu}$ for categorical features. Fix all the variables but those corresponding to one of these features. Since the variables y are integer in an optimal solution, the feasible set of the resulting problem is a simplex, and a basic optimal solution is therefore integer.

2. Model Refinements

In this section, we discuss some additional formulation refinement and extensions. Firstly, we provide improved formulations for ordinal features. Next, we discuss multivariate splits for numerical features and combinatorial splits for categorical features.

Ordinal features. These features involve ordered levels in a similar fashion as numerical features, but open intervals between successive levels bear no meaning or should be prohibited. In this case, no fractional value should arise due to (e.g., actionability or plausibility) side constraints, and the associated costs are typically discretized over the ordinal levels. To efficiently model these features, we use specialized constraints that represent a simplification of the formulation used for numerical features.

Let k_i be the number of possible categories for ordinal feature $i \in I_\text{O}$. For each tree t, let $\mathcal{V}_{tij}^I$ be the set of internal nodes involving a split on feature i at level j, such that samples with feature level smaller or equal to j descend to the left branch, whereas other samples descend to the right branch. Consistency of feature i can be ensured through auxiliary variables ω_i^j for $j \in \{1, \ldots, k_i - 1\}$ which take value 0 if feature i has a level smaller or equal to j and 1 otherwise. These conditions can be ensured as follows:

$$\omega_i^{j-1} \geq \omega_i^j \qquad j \in \{2, \ldots, k_i - 1\} \tag{1}$$

$$\omega_i^j \leq 1 - y_{tl(v)} \qquad j \in \{1, \ldots, k_i - 1\}, t \in \mathcal{T}, v \in \mathcal{V}_{tij}^I \tag{2}$$

$$\omega_i^j \geq y_{tr(v)} \qquad j \in \{1, \ldots, k_i - 1\}, t \in \mathcal{T}, v \in \mathcal{V}_{tij}^I \tag{3}$$

$$\omega_i^j \in \{0, 1\} \qquad j \in \{1, \ldots, k_i - 1\}. \tag{4}$$

Multivariate splits on numerical features. If the need arises, one can also model the search for counterfactual explanations in contexts where some splits of the decision trees (or isolation trees – e.g., as in extended isolation forests) involve linear combinations of the features. To that end, we can rely on big-M constraints as follows:

$$\mathbf{a}_{tv}\mathbf{x} \leq b_{tv} - \epsilon + M_{tv}^+(1 - y_{tL(v)}) \qquad t \in \mathcal{T}, v \in \mathcal{V}_t^I \tag{5}$$

$$\mathbf{a}_{tv}\mathbf{x} \geq b_{tv} + \epsilon - M_{tv}^-(1 - y_{tR(v)}) \qquad t \in \mathcal{T}, v \in \mathcal{V}_t^I. \tag{6}$$

It is important to use the smallest possible value for the big-M constants to achieve a good linear relaxation. Given that numerical features are normalized in the interval $[0, 1]$, we can use:

$$M^+_{tv} = \sum_{k=1}^{p} \max\{0, a_{tvp}\} - b_{tv} \tag{7}$$

$$M^-_{tv} = b_{tv} - \sum_{k=1}^{p} \min\{0, a_{tvp}\}. \tag{8}$$

Combinatorial splits on categorical features. As usual for categorical features, k_i will be used to denote the number of possible categories for feature $i \in I_{\mathrm{C}}$, and let ν_i^j be a variable that will take value 1 if x_i belongs to category $j \in \{1, \ldots, k_i\}$ and 0 otherwise. Combinatorial splits on categorical features involve sending certain categories towards the right branch, and the rest on the left. For each split at an internal node v of tree t, let C^+_{ivt} be the set of categories that descend towards the right branch. Then, the consistency of categorical feature i through the forest with combinatorial splits can be modeled as:

$$\sum_{j \in C^+_{ivt}} \nu_i^j \leq 1 - y_{tl(v)} \qquad t \in \mathcal{T}, v \in \mathcal{V}_t^I \tag{9}$$

$$\sum_{j \in C^+_{ivt}} \nu_i^j \geq y_{tr(v)} \qquad t \in \mathcal{T}, v \in \mathcal{V}_t^I \tag{10}$$

$$\nu_i^j \in \{0, 1\} \qquad j \in C_i \tag{11}$$

$$\sum_{j \in C_i} \nu_i^j = 1. \tag{12}$$

3. Detailed Numerical Results

This section provides additional detailed experimental results complementing those of the main paper.

3.1. Detailed Performance Comparisons

Figures F1 and F2 extends Figures 2 and 3 in the main body of the paper with an analysis on all datasets and methods. In those figures, and missing data point for a method means that no feasible counterfactual has been found (possible for FT due to the way the search process is conducted) or that the CPU time limit of 900 seconds has been exceeded.

The left section of Table A1 extends the results of Table 3 in the main paper for a varying number of trees “#T” in $\{10, 20, 50, 100, 200, 500\}$ with a maximum depth fixed to 5. In a similar fashion, the right section of the table extends these results for varying depth “#D” in $\{3, 4, 5, 6, 7, 8\}$ with a number of trees fixed to 100.

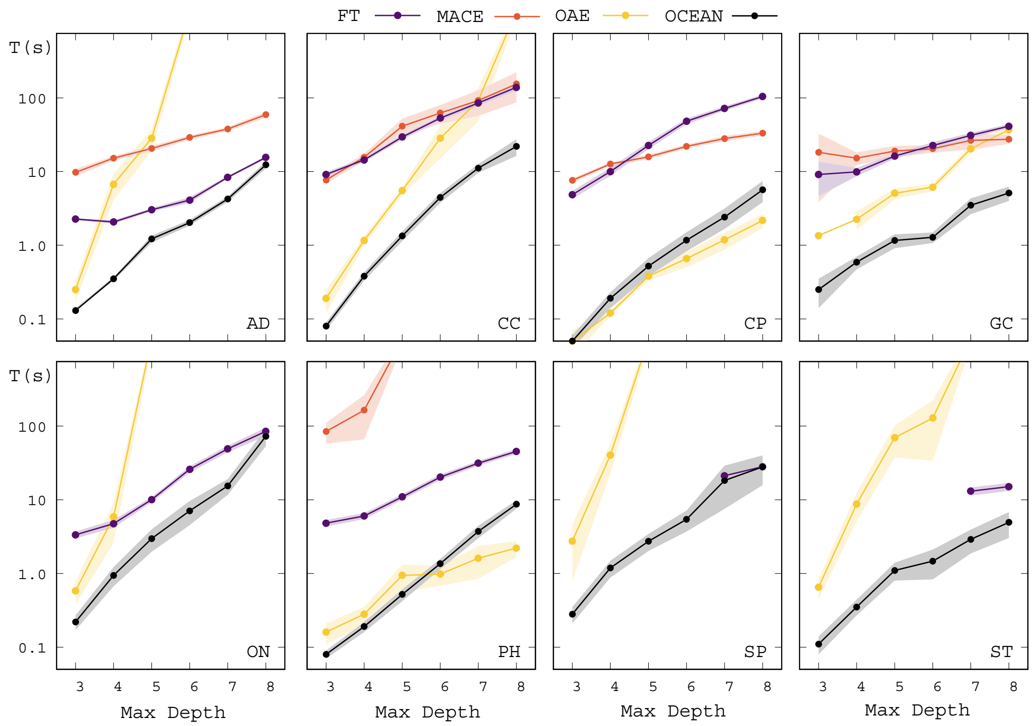

Figure F1. Comparative analysis of CPU time as a function of the maximum depth of the trees – considering all data sets

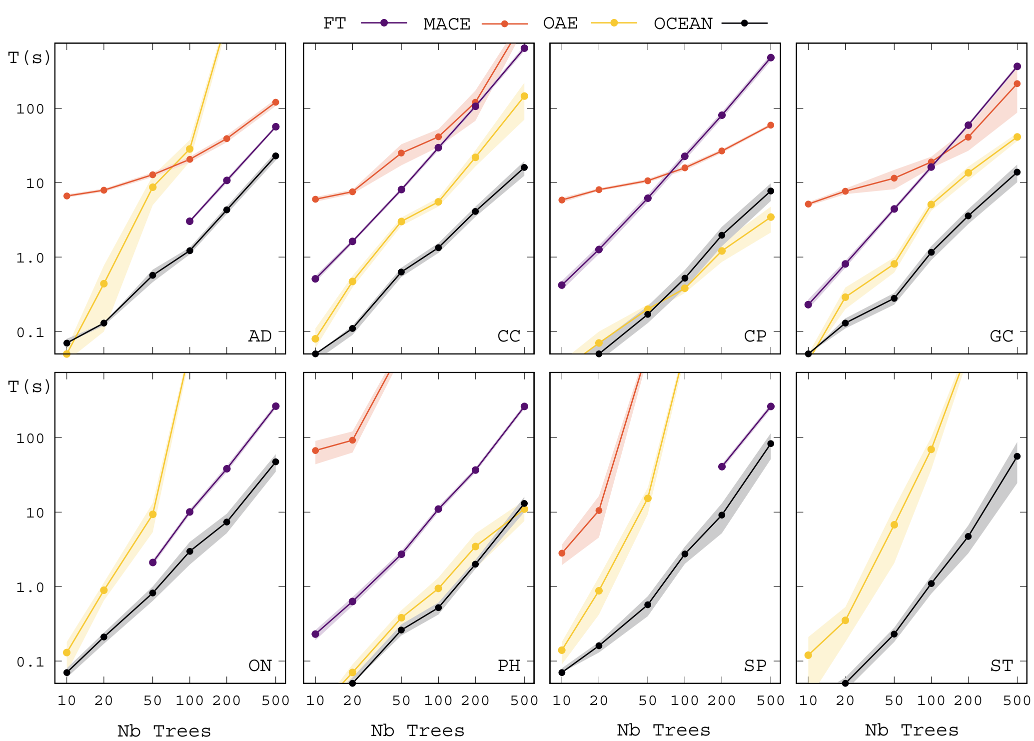

Figure F2. Comparative analysis of CPU time as a function of the number of trees in the ensemble – considering all data sets

Table A1. Time and solution quality comparison, considering all configurations

#T	Data	FT		MACE		OAE		OCEAN	
		T(s)	R	T(s)	R	T(s)	R	T(s)	R
10	**AD**	NA	—	6.64	1.0	0.05	1.0	0.07	1.0
	CC	0.51	23.0	5.99	1.3	0.08	1.0	0.05	1.0
	CP	0.42	18.5	5.85	1.0	0.03	1.0	0.02	1.0
	GC	0.23	17.4	5.17	1.0	0.04	1.0	0.05	1.0
	ON	0.13	106.0	>900	—	0.13	1.0	0.07	1.0
	PH	0.23	1.7	67.13	1.0	0.02	1.0	0.02	1.0
	SP	NA	—	2.80	7.6	0.14	1.0	0.07	1.0
	ST	NA	—	>900	—	0.12	1.0	0.02	1.0
20	**AD**	NA	—	7.92	1.0	0.44	1.0	0.13	1.0
	CC	1.62	22.2	7.56	1.3	0.47	1.0	0.11	1.0
	CP	1.27	10.6	8.07	1.0	0.07	1.0	0.05	1.0
	GC	0.81	10.0	7.69	1.0	0.29	1.0	0.13	1.0
	ON	NA	—	>900	—	0.89	1.0	0.21	1.0
	PH	0.63	1.4	92.15	1.0	0.07	1.0	0.05	1.0
	SP	NA	—	10.51	4.9	0.88	1.0	0.16	1.0
	ST	NA	—	>900	—	0.35	1.0	0.05	1.0
50	**AD**	NA	—	12.80	1.1	8.71	1.0	0.57	1.0
	CC	8.06	5.9	24.97	1.1	3.02	1.0	0.63	1.0
	CP	6.19	5.0	10.65	1.0	0.20	1.0	0.17	1.0
	GC	4.44	6.2	11.51	1.0	0.81	1.0	0.28	1.0
	ON	2.10	97.7	>900	—	9.29	1.0	0.82	1.0
	PH	2.72	1.6	>900	—	0.38	1.0	0.26	1.0
	SP	NA	—	>900	—	15.31	1.0	0.57	1.0
	ST	NA	—	>900	—	6.75	1.0	0.23	1.0
100	**AD**	3.03	15.9	20.60	1.1	28.37	1.0	1.22	1.0
	CC	29.44	10.2	41.25	1.2	5.52	1.0	1.34	1.0
	CP	22.68	4.5	15.82	1.0	0.38	1.0	0.52	1.0
	GC	16.26	4.8	19.03	1.0	5.08	1.0	1.16	1.0
	ON	10.05	31.7	>900	—	>900	—	2.97	1.0
	PH	10.95	1.4	>900	—	0.94	1.0	0.52	1.0
	SP	NA	—	>900	—	>900	—	2.73	1.0
	ST	NA	—	>900	—	69.64	1.0	1.10	1.0
200	**AD**	10.69	14.8	39.18	1.0	>900	—	4.30	1.0
	CC	106.37	8.3	120.31	1.2	21.89	1.0	4.12	1.0
	CP	80.53	3.4	26.61	1.0	1.21	1.0	1.97	1.0
	GC	59.37	4.9	40.91	1.0	13.58	1.0	3.59	1.0
	ON	38.18	18.4	>900	—	>900	—	7.34	1.0
	PH	36.60	1.6	>900	—	3.44	1.0	1.99	1.0
	SP	40.71	8.5	>900	—	>900	—	9.13	1.0
	ST	NA	—	>900	—	>900	—	4.70	1.0
500	**AD**	56.39	18.0	120.25	1.1	>900	—	22.96	1.0
	CC	640.08	4.9	>900	—	145.36	1.0	15.98	1.0
	CP	479.78	2.9	59.36	1.0	3.45	1.0	7.74	1.0
	GC	365.30	4.2	214.64	1.0	41.22	1.0	13.82	1.0
	ON	265.22	33.0	>900	—	>900	—	47.35	1.0
	PH	261.96	1.5	>900	—	10.96	1.0	13.05	1.0
	SP	262.35	7.7	>900	—	>900	—	83.05	1.0
	ST	NA	—	>900	—	>900	—	55.95	1.0

#D	Data	FT		MACE		OAE		OCEAN	
		T(s)	R	T(s)	R	T(s)	R	T(s)	R
3	**AD**	2.27	22.6	9.76	1.0	0.25	1.0	0.13	1.0
	CC	9.13	128.2	7.69	6.1	0.19	1.0	0.08	1.0
	CP	4.86	5.9	7.59	1.0	0.05	1.0	0.05	1.0
	GC	9.14	1.9	18.27	1.0	1.35	1.0	0.25	1.0
	ON	3.35	38.5	>900	—	0.58	1.0	0.22	1.0
	PH	4.82	1.3	84.46	1.0	0.16	1.0	0.08	1.0
	SP	NA	—	>900	—	2.74	1.0	0.28	1.0
	ST	NA	—	>900	—	0.65	1.0	0.11	1.0
4	**AD**	2.07	22.5	15.19	1.0	6.71	1.0	0.35	1.0
	CC	14.40	26.5	15.66	1.4	1.16	1.0	0.38	1.0
	CP	10.00	4.9	12.68	1.0	0.12	1.0	0.19	1.0
	GC	9.92	5.2	15.21	1.0	2.25	1.0	0.59	1.0
	ON	4.74	52.1	>900	—	5.86	1.0	0.94	1.0
	PH	6.02	1.5	164.22	1.0	0.28	1.0	0.19	1.0
	SP	NA	—	>900	—	40.31	1.0	1.19	1.0
	ST	NA	—	>900	—	8.76	1.0	0.35	1.0
5	**AD**	3.03	15.9	20.60	1.1	28.37	1.0	1.22	1.0
	CC	29.44	10.2	41.25	1.2	5.52	1.0	1.34	1.0
	CP	22.68	4.5	15.82	1.0	0.38	1.0	0.52	1.0
	GC	16.26	4.8	19.03	1.0	5.08	1.0	1.16	1.0
	ON	10.05	31.7	>900	—	>900	—	2.97	1.0
	PH	10.95	1.4	>900	—	0.94	1.0	0.52	1.0
	SP	NA	—	>900	—	>900	—	2.73	1.0
	ST	NA	—	>900	—	69.64	1.0	1.10	1.0
6	**AD**	4.11	21.6	29.08	1.1	>900	—	2.03	1.0
	CC	53.13	11.5	62.36	1.2	28.33	1.0	4.45	1.0
	CP	48.20	9.1	21.96	1.0	0.66	1.0	1.17	1.0
	GC	22.60	6.9	20.41	1.0	6.15	1.0	1.28	1.0
	ON	25.94	24.7	>900	—	>900	—	7.08	1.0
	PH	20.30	1.3	178.61	1.0	0.98	1.0	1.36	1.0
	SP	NA	—	>900	—	>900	—	5.42	1.0
	ST	NA	—	>900	—	128.52	1.0	1.47	1.0
7	**AD**	8.38	22.3	37.84	1.1	>900	—	4.24	1.0
	CC	85.39	13.6	92.11	1.2	92.18	1.0	11.13	1.0
	CP	71.92	8.2	28.14	1.0	1.18	1.0	2.41	1.0
	GC	30.99	7.7	26.50	1.0	20.41	1.0	3.49	1.0
	ON	49.16	70.9	>900	—	>900	—	15.41	1.0
	PH	31.33	1.3	>900	—	1.61	1.0	3.72	1.0
	SP	21.22	7.8	>900	—	>900	—	18.26	1.0
	ST	13.07	3.3	>900	—	>900	—	2.91	1.0
8	**AD**	15.55	10.5	59.30	1.1	>900	—	12.35	1.0
	CC	139.40	18.2	154.47	1.3	>900	—	21.96	1.0
	CP	104.49	9.1	33.11	1.0	2.17	1.0	5.65	1.0
	GC	41.25	7.5	27.45	1.0	36.89	1.0	5.11	1.0
	ON	84.72	60.3	>900	—	>900	—	72.87	1.0
	PH	45.32	1.3	236.58	1.0	2.21	1.0	8.70	1.0
	SP	28.16	6.7	>900	—	>900	—	27.94	1.0
	ST	15.07	3.0	>900	—	>900	—	4.93	1.0

3.2. Detailed Performance with Plausibility Constraints

This section provides additional detailed results concerning the performance of OCEAN with plausibility constraints via isolation forests.

Firstly, Figure F3 displays the same computational time analysis as Figure 1 in the main paper, when considering the additional plausibility constraints through isolation forests. As visible on this figure, OCEAN maintains a good scalability for all objectives even with the plausibility restrictions.

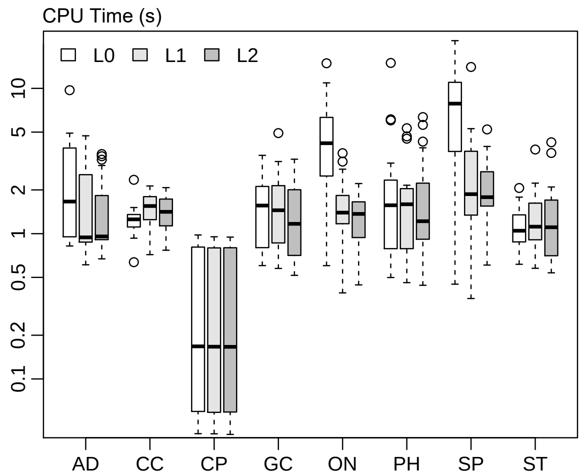

Figure F3. CPU time to find an optimal counterfactual explanations, considering different data sets and objectives

Finally, Table A2 reports the average computational time in seconds needed to find optimal counterfactual explanations with (OCEAN-IF) and without (OCEAN-noIF) plausibility constraints as a function of the maximum depth of the trees (in $\{5, 6, 7, 8\}$, corresponding to a maximum of $\{32, 64, 128, 256\}$ leaves). In these experiments, we use the l_1 objective, the number of trees is set to the baseline value of 100, and the isolation forest has the same depth limit as the random forest.

Table A2. CPU time (s) of OCEAN with isolation forests for ensuring plausibility

Data set	**OCEAN-noIF**				**OCEAN-IF**			
Max-Depth	5	6	7	8	5	6	7	8
Max-Leaves	32	64	128	256	32	64	128	256
AD	0.75	1.43	2.70	5.36	1.82	3.83	7.26	14.10
CC	0.99	4.70	9.14	24.50	1.54	5.42	12.83	32.83
CP	0.44	1.18	2.74	5.32	0.85	1.35	3.18	7.06
GC	0.60	1.15	2.05	3.50	1.71	3.59	11.04	18.16
ON	1.34	3.19	9.61	36.81	1.64	4.29	11.79	41.87
PH	0.36	1.16	2.25	5.09	1.81	5.86	15.16	43.12
SP	2.71	6.60	15.92	34.02	4.43	7.18	27.63	37.98
ST	0.62	1.47	2.22	3.13	1.36	3.63	8.13	12.31

As visible in these experiments, the use of the plausibility restrictions through isolation forests roughly doubles the time needed to locate optimal explanations. This increase directly relates to the fact that considering both the random forest and isolation forest simultaneously involves considering twice the number of trees. Despite this increase of model complexity, optimal explanations are found in less than one minute, even when considering a maximum depth of 8 (i.e., with up to 256 leaves per tree and $51,200$ leaves overall in both forests).

4. Open Source Code

All the material (source code and data sets) needed to reproduce our experiments is accessible at `https://github.com/vidalt/OCEAN` under a MIT license.